Accepted Manuscript

Novel parameter-based flexure bearing design method

Simon Amoedo, Edouard Thebaud, Michael Gschwendtner, David White

Novel parameter-based flexure bearing design method
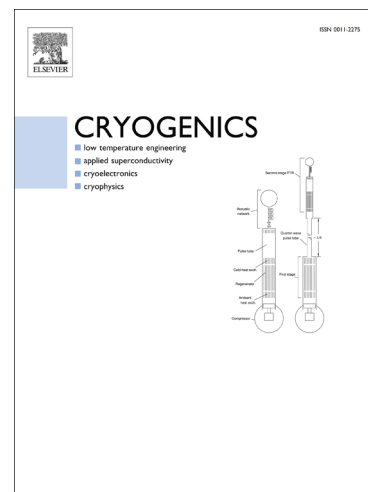
Simon Amoedo[1], Edouard Thebaud[1], Michael Gschwendtner[2] and David White[2]

[1]ISAE-ENSMA, France

[2]Department of Mechanical Engineering, Mathematical & Computer Sciences, Auckland University of Technology, New Zealand

Corresponding author:

Michael Gschwendtner, School of Engineering, Mathematical and Computer Sciences, Auckland University of Technology, Private Bag 92006, Auckland 1142, New Zealand.
Email: michael.gschwendtner@aut.ac.nz

Highlights

• Modal analysis of different flexure bearing configurations is performed.

• Dynamic tests on the flexure bearing are carried out using Finite Element Method.

• Parametric studies of the influence geometric dimensions have on bearing performance.

• Development of a graphical design tool that identifies optimal flexure bearing configuration.

Abstract

A parameter study was carried out on the design variables of a flexure bearing to be used in a Stirling engine with a fixed axial displacement and a fixed outer diameter. A design method was developed in order to assist identification of the optimum bearing configuration. This was achieved through a parameter study of the bearing carried out with ANSYS®. The parameters varied were the number and the width of the arms, the thickness of the bearing, the eccentricity, the size of the starting and ending holes, and the turn angle of the spiral. Comparison was made between the different designs in terms of axial and radial stiffness, the natural frequency, and the maximum induced stresses. Moreover, the Finite Element Analysis (FEA) was compared to theoretical results for a given design. The results led to a graphical design method which assists the selection of flexure bearing geometrical parameters based on pre-determined geometric and material constraints.

Keywords

Flexure bearing, finite element method, parameter study, Stirling engine, design method.

Nomenclature

c_x Stress-raising factors

d diameter of the starting and ending holes, m

f_{nat} natural frequency of the bearing, Hz

F_x axial force, N

F_y radial force, N

ID active inner active diameter, m

ID' physical inner diameter, m

k_a axial stiffness, N/m

k_r radial stiffness, N/m

n number of arms, m

OD active outer active diameter, m

OD' physical outer diameter, m

p pitch

r_0 radius at the beginning of the spiral, m

s slot width, m

S_e Endurance limit of flexure bearing, MPa

S'_e Endurance limit of rotating beam specimen, MPa

t thickness of the disk, m

w arm width, m

δ_x axial displacement, m

δ_y radial displacement, m

Δx displacement, mm

Θ turn angle, degrees

σ_{max} axial maximum stress, Pa

1. Introduction

Flexure bearings are metal disks with spiral-like slots that enable them to flex in axial direction while exhibiting a much higher radial stiffness. They can be used to support shafts that perform a pure linear motion and are commonly used in free-piston Stirling machines in combination with linear motors. In these applications, their primary advantage is almost frictionless operation without requiring lubrication. They can be used in combination with clearance seals; they are inexpensive and can be easily manufactured by a dye in a punch press.

The concept of a flexure bearing or flexure spring was first introduced and patented by A. Wolf et al. in 1938 [1]. They used these bearings, mounted in a vibration detector, to capture the Earth's vibrations. Then, in 1981, flexure bearings were first used in a Stirling cryocooler at the University of Oxford [2]. Later, in 1992, Wong et al. [3] optimised a three-spiral flexure bearing using Finite Element Method (FEM) which was subsequently experimentally validated. These researchers also showed that the radial stiffness decreases with axial displacement and that the maximum stresses occur at the end of the spiral slot. In the same year, Marquardt et al. [4] proposed a design correlation for flexure bearings where the ratio of radial to axial spring stiffness was used to select the most suitable configuration for their application. The use of correlations in flexure bearing design was further developed by Wong et al. [5], who, in 1995, performed static and dynamic tests using FEM on a three-spiral slot flexure bearing. Their model results, verified through experimental dynamic testing, recommended that the dynamic stresses, rather than the static ones, be used for the fatigue analysis.

In 1996, Gaunekar et al. [6] analysed a three-spiral flexure bearing using FEA and found that the stresses increase with the axial displacement. Furthermore, they found that the axial and radial stiffness tend to have a linear behaviour when plotted against the axial displacement. They also noticed that the bearing's axial and radial stiffness also increases with increasing bearing material thickness. This work resulted in normalised graphs that assist in flexure bearing design.

Automated geometry creation for a three-spiral flexure bearing within Fortran was later achieved by varying the turn angle, thickness, and the outside radius. This work, undertaken by C. C. Lee and R. B. Pan [7], automated design generation and demonstrated that there were many design possibilities for a given low radial stiffness, but fewer for a high stiffness.

More recently, in 2007, Z. S. Al-Otaibi and A. G. Jack [8] designed a flexure bearing for a linear-resonant motor with experimental validation of the FE results. Their findings suggested that an increase in turn angle of the spiral decreases the stresses and the axial stiffness, while the axial stiffness increases with the thickness of the disk. These findings

were later supported by C.J. Simcock [9] who studied a flexure spring using FEM and performed experimental tests using strain gauges to measure bearing stresses. In 2012, S. Malpani et al. [10] and M.V.Kavade et al. [11] performed a similar FEM study on a flexure bearing by varying the turn angle of the spiral and the thickness of the bearing. They also validated their results experimentally and found good agreement with their earlier work.

The purpose of this investigation is to test different parameters of a spiral flexure bearing design and analyse their influence in terms of fatigue when applied to a flexure bearing. The parameter study presented here indicates which parameters can be varied and what their impact is on bearing performance. In this study, parameters were varied that have not been analysed before, such as the size of the ending holes or the number of arms. This investigation also uses the stiffness ratio, originally introduced by Marquardt et al. [4] as a theoretical concept, to compare the different configurations under dynamic load. This ratio has not previously been used to compare several bearing designs obtained by using FEM. Furthermore, a modal analysis of the flexure bearing is also carried out using FEM. The dynamic stresses on the bearing are then analysed and minimised for a given design. Finally, as a result of the parameter study, a design method is developed in order to select the optimum geometric configuration of the bearing depending on pre-selected geometric and material design constraints. Large deflections effects for the displacements have been taken into consideration during the FE simulations in ANSYS®.

2. Geometry and definitions

This investigation considers the variation of geometric parameters, such as the thickness t of the disk, the number of arms n, the turn angle Θ, the diameter of the starting and ending holes d, and the slot width s that determines the arm width w, for a fixed active outer and inner diameter OD and ID, defined as the area that experiences flexure, a fixed stroke, and a fixed radius r_0 at the beginning of the spiral. The flexure bearing considered here had an outer diameter of OD' 90 mm, an active diameter OD of 80 mm, an active inner diameter ID of 20 mm, and a radius r_0 at the beginning of the spiral of 10 mm (Figure 1). Also, a centre hole ID' (the inner diameter) with 8 mm diameter provided space for the shaft of the Stirling engine. Its design is based on the Archimedean spiral as described by Al-Otaibi [8]. The flexure bearing analysed has three arms (n = 3), the spirals make 1 turn (Θ = 360°), the arm width w is set to 9.33 mm (for a 0.5 mm slot width s), and the thickness t of the disk is 0.7 mm. Also, the starting and ending holes of the spiral are set to a 1.5 mm diameter d.
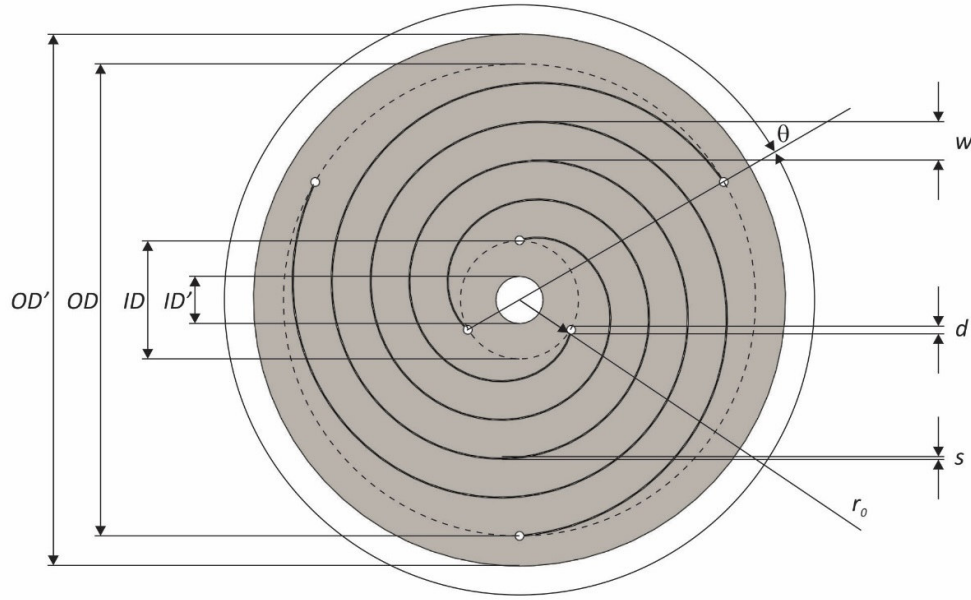
Figure 1: The geometric parameters of the flexure bearing analysed in this study. The dashed circles mark the boundaries of the area that experiences flexure.

3. **Finite element analysis**

3.1. *Varying the turn angle and number of arms*

The first parameters investigated in this paper were the turn angle of the spirals and the number of arms. The turn angle Θ was varied from 360° to 1080° in 90° increments, while the number of arms n were 2, 3, and 4. For this analysis the thickness of the bearing was 0.7 mm.

Once assembled in the engine, the bearing will oscillate at a specific frequency. In order to determine the permissible operating frequency, a modal analysis has to be carried out to find the natural frequency of the bearing in order to avoid the destructive consequences of resonance.

For this analysis, the displacement of the central area was held unconstrained in the axial direction, while the outer rim was fixed to meet the real boundary conditions. These conditions are shown in Figure 2 where the shaded area around the centre hole is free to move in axial direction, while the shaded area at the outer rim is fixed.
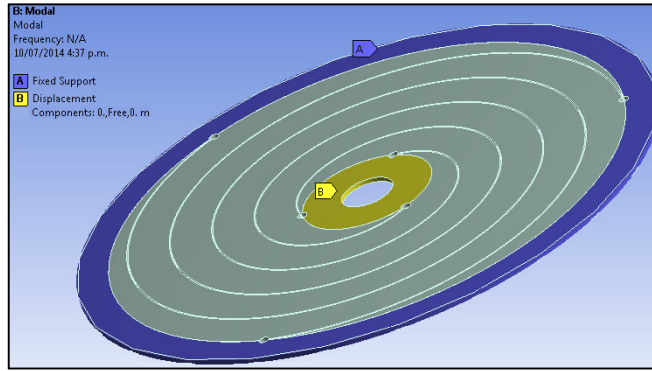
Figure 2: Boundary conditions for the modal analysis.

These conditions were used for both the radial and axial tests. In the first case, a static bearing load was applied radially at the centre hole at zero stroke while a dynamic force was applied axially in the second test. In both cases the outer rim remained fixed. The material chosen for all the analyses was AISI 5160 which has the same characteristics as the materials used for metal springs (i.e. stainless steel with high yield strength), with a Young's modulus of 210 GPa, a Poisson's ratio of 0.29, and a density of 7850 kg/m^3.

Figure 3 shows the mesh used for the analysis conducted with ANSYS 15. The meshing parameters were set to have a great number of elements at the starting holes of the spirals, where the stresses are expected to be concentrated.
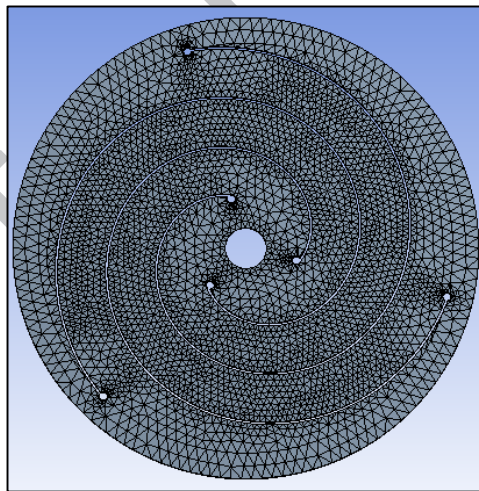
Figure 3: Mesh of the flexure bearing.

Resonance causes unexpected motions on the bearing that can lead to premature failure if the operating frequency is near the natural frequency. In order to avoid this situation, an operating frequency below the natural frequency was selected for the subsequent analysis within this study. Comparison between the results of the modal analysis and those given by Wahl's correlation [12], shown in Figure 4, shows that the natural frequency decreases with increasing turn angle and increasing number of arms, however, with a much stronger

6

influence of the turn angle. It can be noticed that there is a good correlation between Wahl's correlations [12] and FE results.
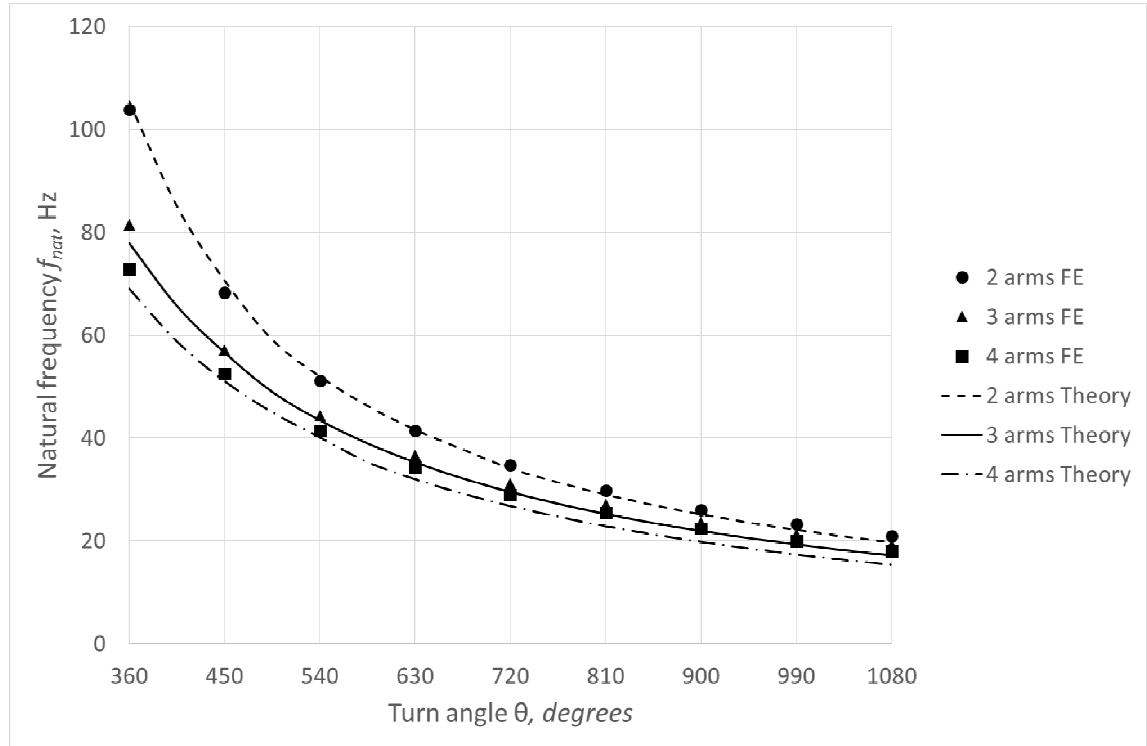

Figure 4: Natural frequency vs turn angle for different numbers of arms.

Subsequently, a dynamic load was applied axially at the centre of the bearing to achieve a 10 mm displacement of the central area at a frequency of 15 Hz. The FE analysis of the radial test was performed for a bearing load of 10 N. With the results of these two tests, the axial and radial stiffness can be calculated as

$$k_a = F_x/\delta_x \quad \text{and} \quad k_r = F_y/\delta_y. \tag{1}$$

Figure 5 shows that the axial stiffness obtained in the FE analysis agrees well with that calculated by Wahl's correlation for turn angles above 450°. Below this value, however, theory underestimates the axial stiffness. Furthermore, the dynamic load required for a 10 mm displacement increases with lower turn angles and fewer arms.
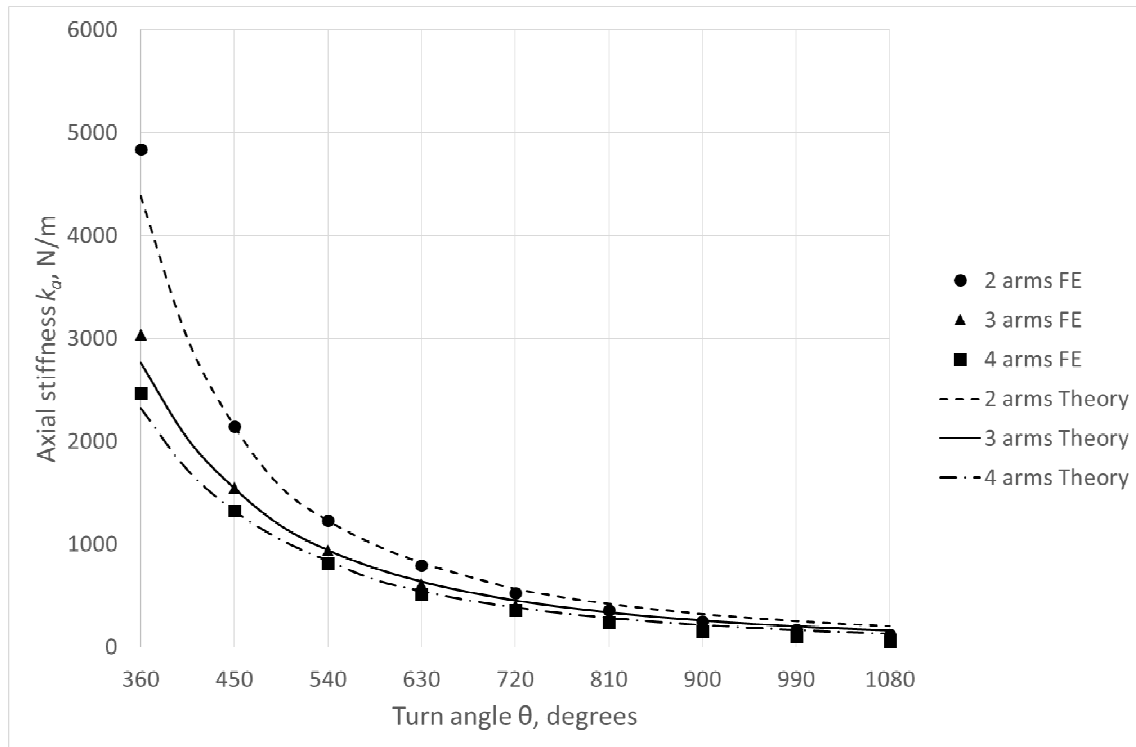
Figure 5: Axial stiffness vs turn angle, theory and FE results.

In terms of the radial stiffness, shown in Figure 6, the theoretical values agree well with the FE predictions above turn angles of 450°.
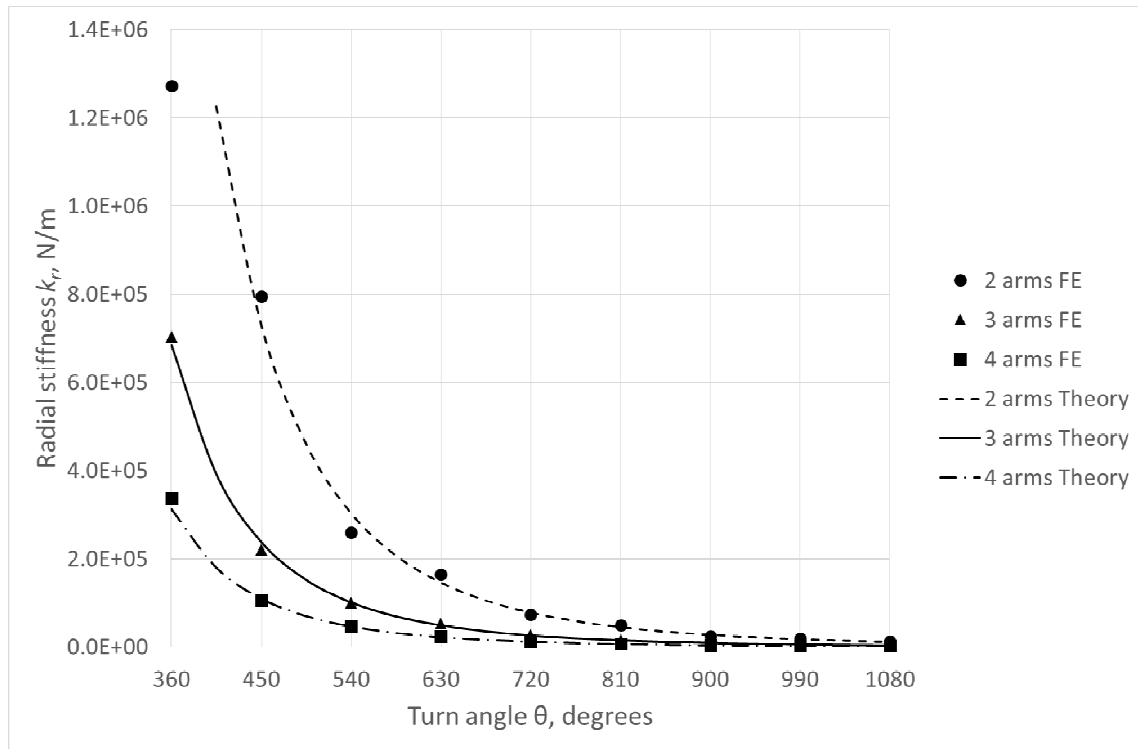
Figure 6: Radial stiffness vs turn angle, theory and FE results.

Flexure bearings require a high radial stiffness k_r and a low axial stiffness k_a to effectively operate. For comparison of the different designs, the k_r over k_a ratio was considered. This stiffness ratio, shown in Figure 7, decreases with increasing turn angle of the spiral, however, it decreases with the number of arms. Again, there is good agreement between the theoretical values and the FE results, even for small turn angles.

9
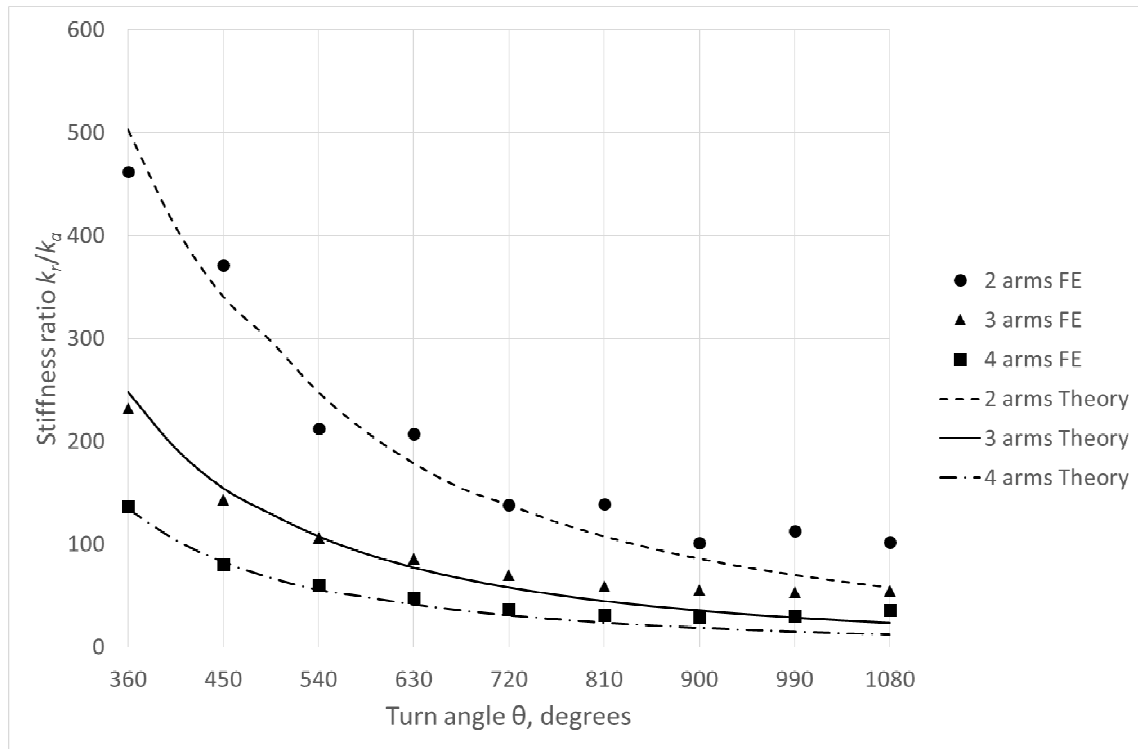
Figure 7: k_r/k_a ratio vs the turn angle for different numbers of arms, theory and FE results.

The maximum induced stresses are critical design parameters, given the desire for infinite flexure bearing life and the potential difficulty to replace them once mounted in the machine. The FE results, Figure 8, show the Von Mises stress distribution on the flexure bearing for the dynamic axial test. Here, the maximum stresses are concentrated at the ending holes of the spirals. This was also found by Wong et al. in their earlier investigation [3].

Configuration	
Arms (n)	3
Turn angle (Θ)	720°
Thickness (t)	0.7 mm
Slot width (s)	0.5 mm
Starting hole diameter (d)	1.5 mm
Force (F_x)	4.2 N
Frequency (f)	15 Hz
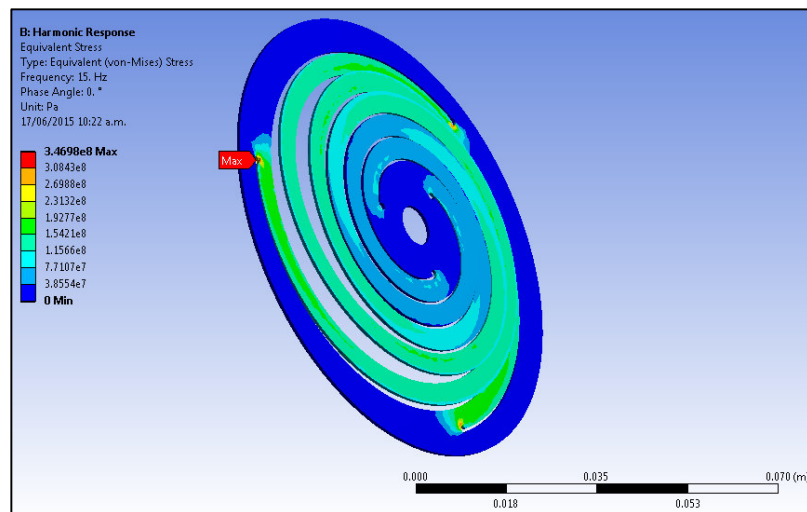
Figure 8: Stress distribution in given configuration.

10

The maximum stresses induced by axial displacement in all the bearing configurations considered in this investigation are plotted in Figure 9. It can be seen that the stresses decrease exponentially with larger values of the turn angle θ and with increasing numbers of arms. This behaviour was also predicted by Z. S. Al-Otaibi et al. in their earlier investigation [8].
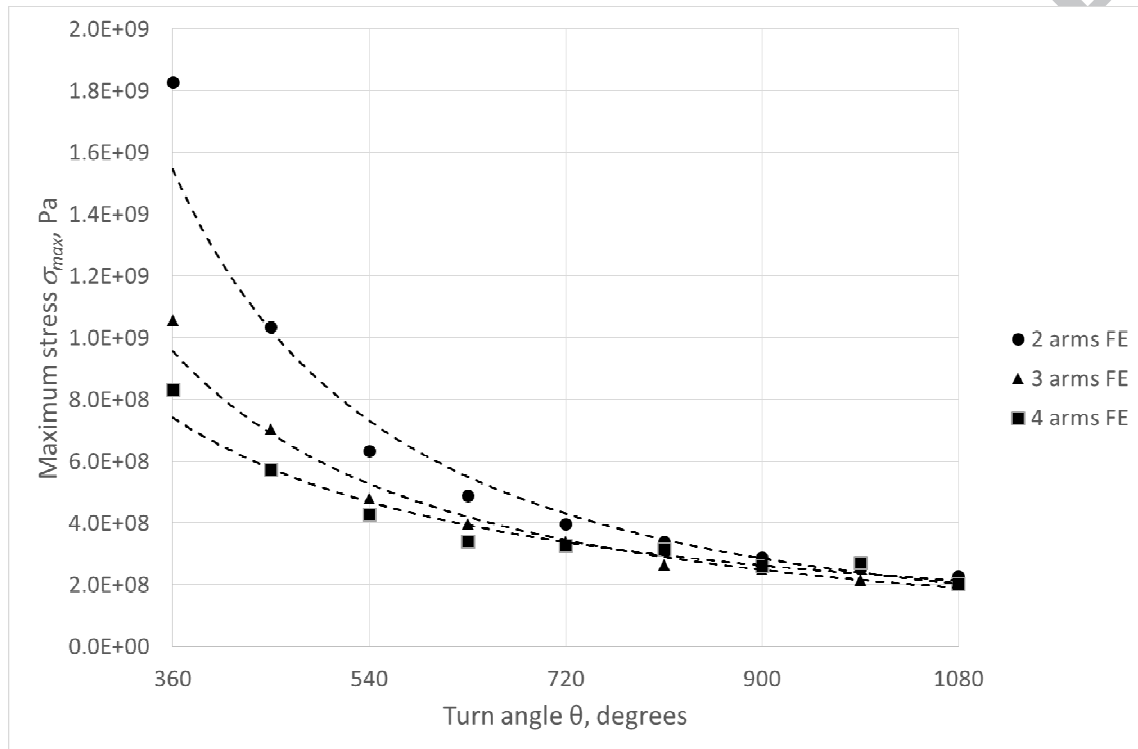
Figure 9: Maximum stress vs turn angle for different numbers of arms (the dashed lines represent curve fits).

3.2. *Variation of the bearing arm width*

Here, the number of arms, the turn angle θ and the thickness were held constant. The tests and the boundary conditions were the same as in earlier testing (Table 1). Under these conditions, the slot width was varied from 0.2 mm to 1.2 mm which corresponds to an arm width which can be obtained directly from the slot width s and the pitch p, which is set at p = 12 mm, by

$$w = p/n - s \tag{2}$$

as listed in Table 2.

Table 1: Fixed parameters of configuration investigated

Configuration	
Arms (*n*)	3
Turn angle (*Θ*)	630°
Thickness (*t*)	0.7 mm
Pitch (*p*)	12 mm
Starting hole diameter (*d*)	2.0 mm
Displacement (δ_x)	10 mm
Frequency (*f*)	15 Hz

Slot width (*s*)	0.2 mm	0.4 mm	0.6 mm	0.8 mm	1 mm	1.2 mm
Arm width (*w*)	5.5 mm	5.3 mm	5.0 mm	4.8 mm	4.5 mm	4.3 mm

Table 2: Corresponding arm width

The theoretical results of the radial stiffness vs the arm width, Figure 10, show a similar trend to those found by FE analysis in that the stiffness increases almost linearly with increasing arm width. Of note is that the discrepancy between the theory and the FE analysis increases for lower arm width values. Also, the theoretical axial stiffness, Figure 11, tends to be underestimated when compared to the FE results, and again, the discrepancy increases with smaller arm widths.
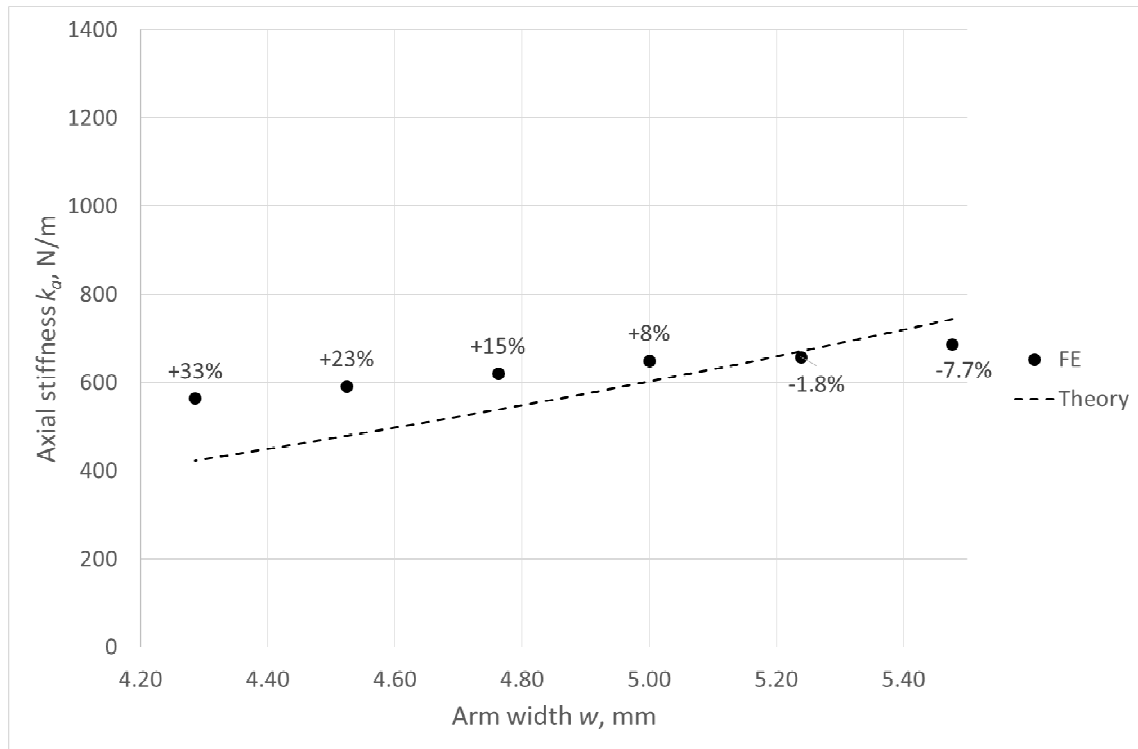
Figure 10: Axial stiffness vs arm width, theory and FE results.
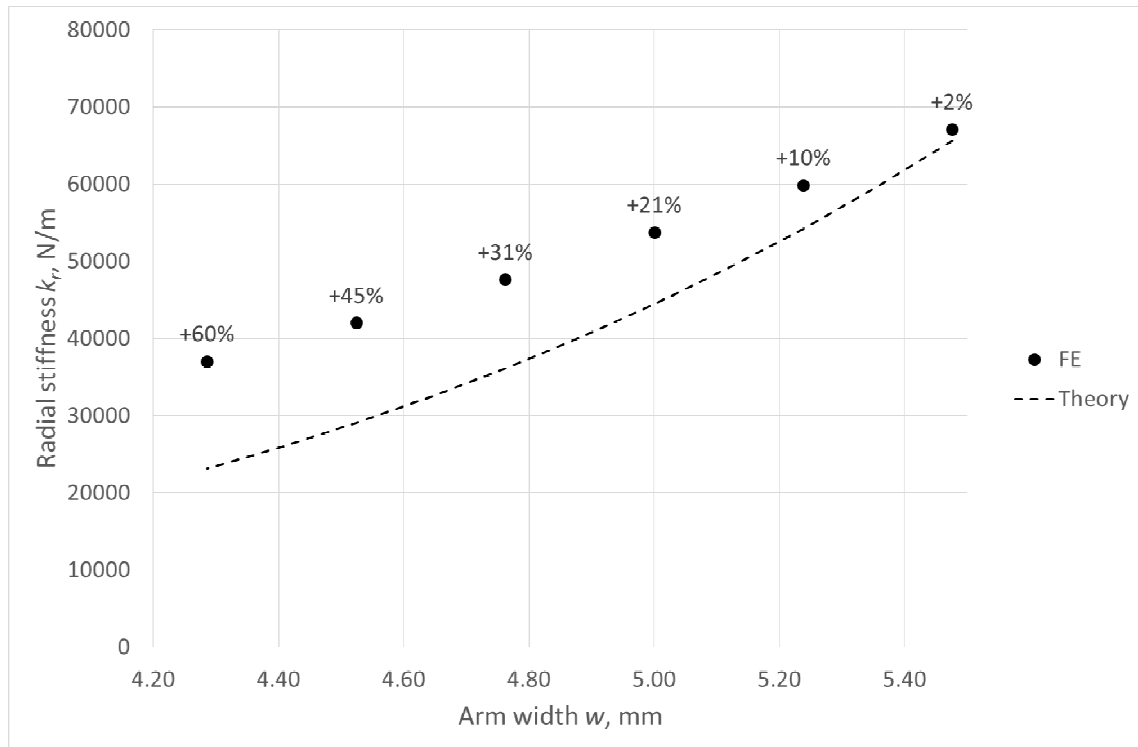
Figure 11: Radial stiffness vs arm width, theory and FE results.

The change of the stiffness ratio with increasing arm width is displayed in Figure 12. Here, as the arm width increases, the stiffness ratio also increases in almost a linear fashion. However, the theory underestimates the FE results and is offset by almost 10%. The natural frequency, however, stays steady at 24.5 Hz for all arm widths tested as noticed during the FE analysis.
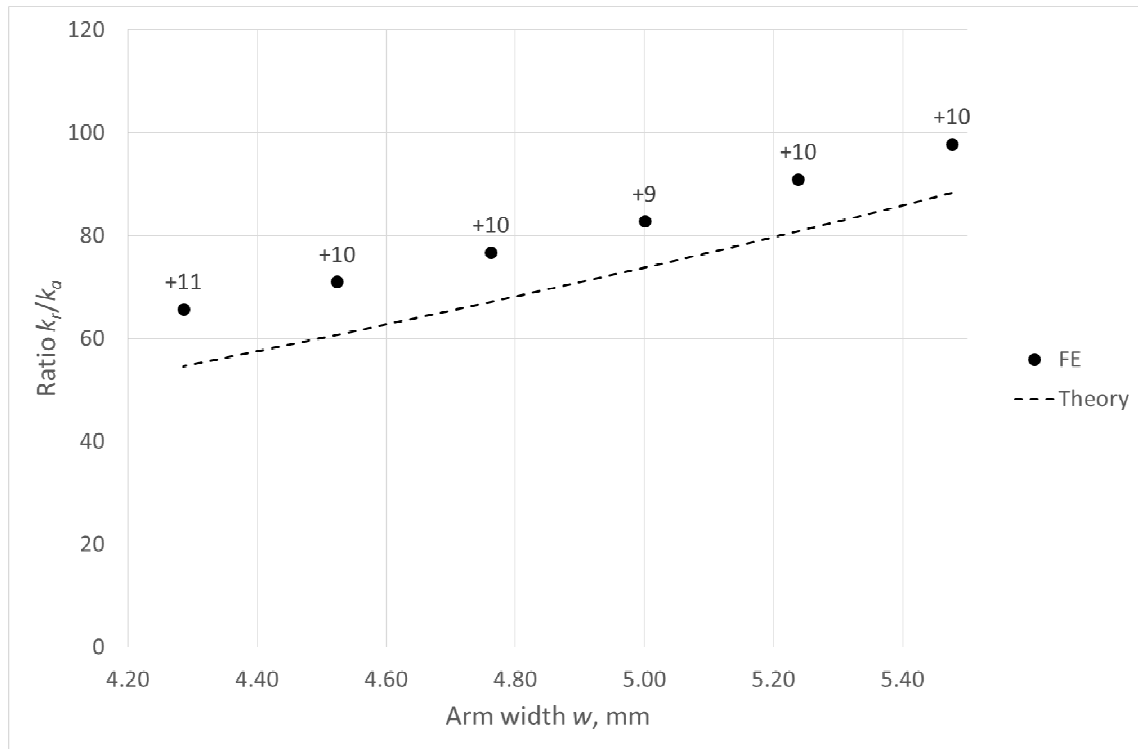
Figure 12: k_r/k_a ratio vs arm width, theory and FE results.

As expected, the Von Mises stresses are higher when the arm width increases (Figure 13) which is due to the fact that a larger force is required to achieve a 10 mm displacement of the centre area of the flexure bearing due to the higher stiffness.

Figure 13: Von Mises maximum stress for the axial test vs arm width.
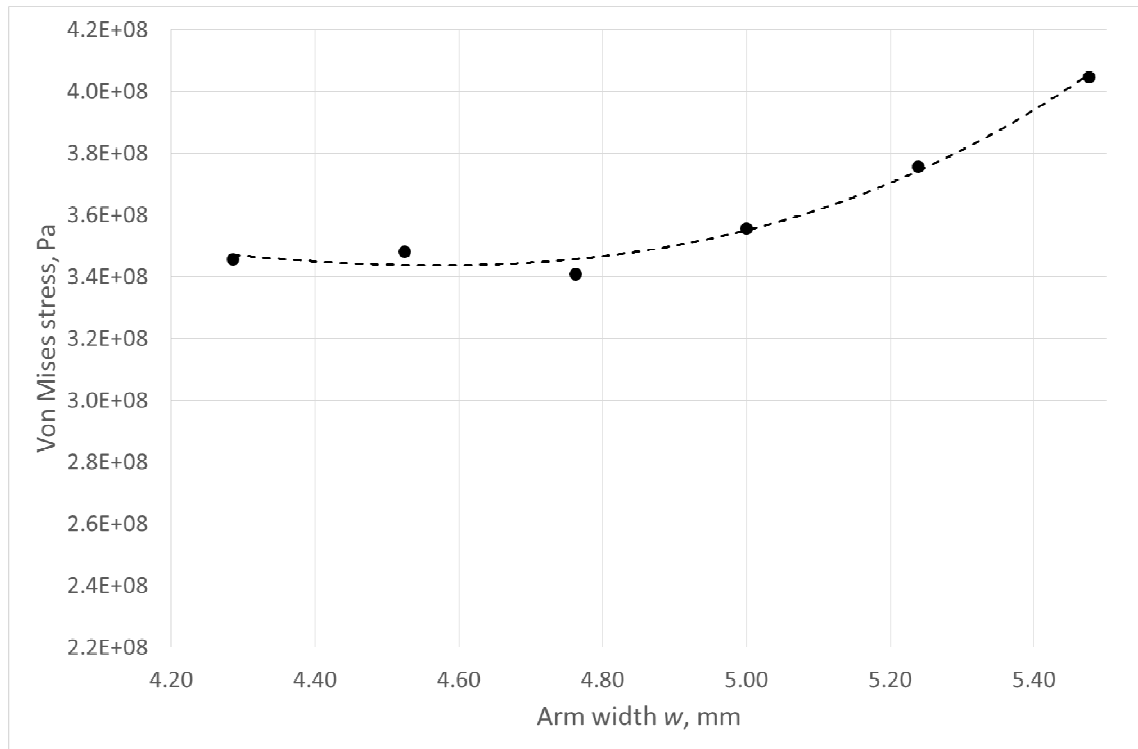
3.3. *Varying the bearing thickness*

Previously the bearing thickness was set to a fixed value of 0.7 mm, however, the variation of this parameter was also investigated. The flexure bearing geometry selected for this analysis consists of 3 arms, a turn angle of 540°, and a 6.1 mm arm width. Again, a dynamic force was applied at a frequency of 15 Hz. Results from the FE analysis show that the axial stiffness and the natural frequency increase with increasing bearing thickness. Additionally, when the k_r/k_a ratio is considered, the thinnest bearings exhibit the highest stiffness ratios as shown in Figure 14. This result agrees with what was found by Gaunekar et al. in their earlier investigation [6]. Also, good agreement between the theoretical and the FE values of the k_r/k_a ratio was found.

16

Configuration	
Arms (*n*)	3
Turn angle (*Θ*)	540°
Arm width (*w*)	6.1 mm
Pitch (*p*)	19.7 mm
Starting hole diameter (*d*)	2.0 mm
Displacement (δ_x)	10 mm
Frequency (*f*)	15 Hz
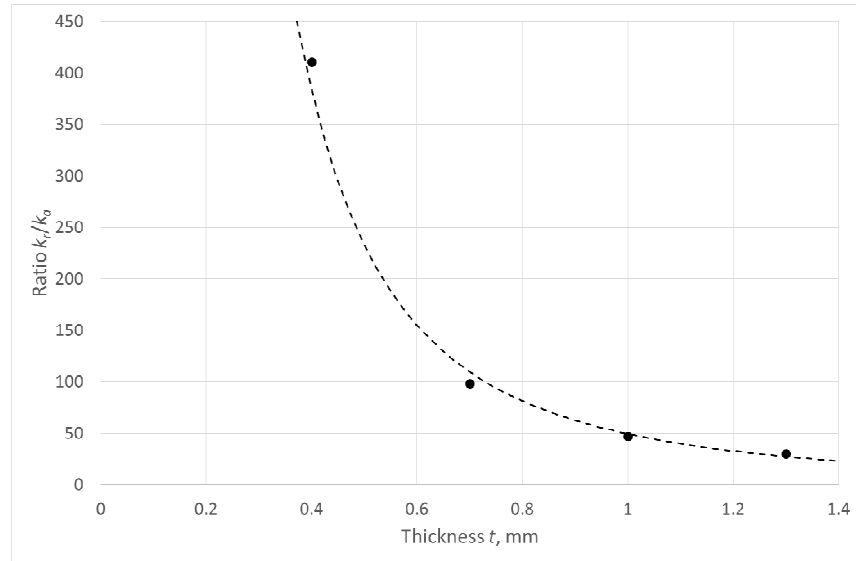
**Figure 14:** FE results of stiffness ratio k_r/k_a vs thickness of the flexure bearing.

3.4. *Varying bearing end of slot hole sizes*

Finally, another FE analysis was carried out to investigate how best to minimise the stress concentration experienced at the starting holes. For this study, the diameter of the ending holes was varied from 1 mm to 6 mm. During this part of the investigation, the flexure bearing had 3 arms, a 6.42 mm arm width (0.2 mm slot width), a 0.5 mm thickness and a turn angle of 540°. The dynamic load was applied at 15 Hz frequency. The maximum Von Mises stresses on the bearing are plotted over a range of hole sizes in Figure 15.

The results show that a minimum in stress occurs at around the 4-5 mm diameter range to stress values of 440 MPa to 340 MPa. It should be noted that this optimal value of the diameter hole is valid only for the design tested. An interesting observation was that the variation of the hole diameters did not significantly change the performance of the flexure bearing in terms of stress ratio or natural frequency. Also, the location of the maximum stress did not change. The hole diameter appears to be a useful parameter to reduce the peak stress occurring at the ending holes.

17

Configuration	
Arms (*n*)	3
Turn angle (*Θ*)	540°
Thickness (*t*)	0.5 mm
Arm width (*w*)	6.42 mm
Displacement (δ_x)	10 mm
Frequency (*f*)	15 Hz
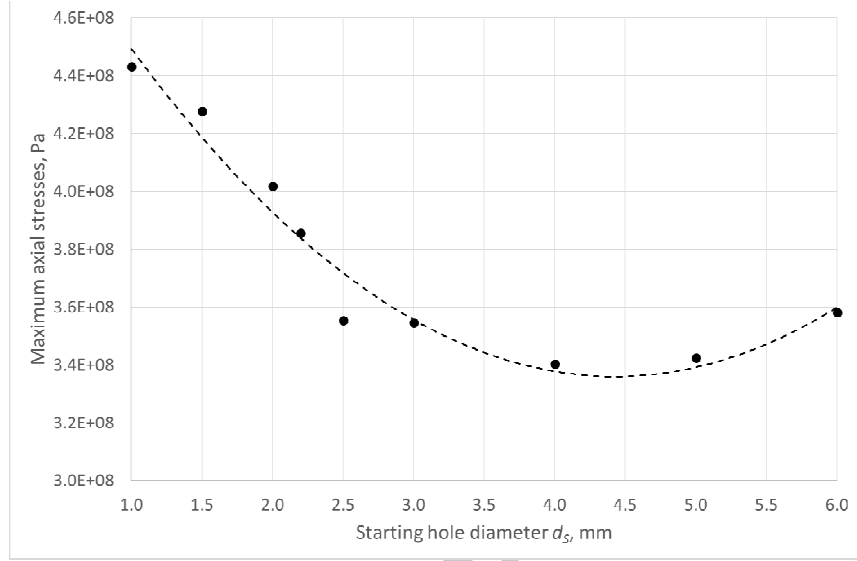
Figure 15: Von Mises stresses during an axial test on the bearing vs the diameter of the starting holes.

4. **Optimal bearing specifications**

4.1. *Fatigue analysis*

As mentioned above, it is desirable that a flexure bearing in a Stirling engine application has a high radial stiffness with a low axial stiffness (i.e. a high stiffness ratio). The bearing must also have a theoretically infinite endurance life. The fatigue analysis for the flexure bearing was done following a standard procedure by multiplying the endurance limit of a rotating beam specimen with a number of stress-raising factors [14]:

$$S_e = c_a c_b c_c c_d c_e S'_e \tag{3}$$

where S_e is the endurance limit of the flexure bearing, S'_e is the endurance limit of the rotating beam specimen, and c_x are the various stress-raising constants. The constants c_x were determined through the use of charts [14] and are independent of the material except for c_a. S'_e depends on the material selected, however, it is constant for materials with a tensile strength above 1380 MPa. For these materials the c_a factor is also constant. So, for materials with an ultimate tensile strength above 1380 MPa (which holds for most stainless steels) a maximum fatigue stress value of 366 MPa was chosen in order to obtain an infinite bearing fatigue life. This ultimate tensile strength was used in this investigation as a reference in all simulations performed and curves plotted. However, due to the linear

relationship between displacement and stress below design method can be used for any other material.

4.2. New *graphical design tool*

Optimising a flexure bearing for application-specific geometric and material constraints takes time and requires a large number of finite elements simulations. A graphical design process was therefore developed based on this study to facilitate the task of selecting bearing characteristics in order to achieve the highest possible stiffness ratio for infinite life. In developing this design tool, the set parameters are rendered dimensionless. Then, applying both the theoretical formulae and finite elements results previously presented by this investigation, a series of graphs can be generated allowing the designer to sequentially select each geometric dimension after another.

The characteristics of a bearing can be divided into two categories – the user's parameters and the designer's parameters. The user's parameters are the boundary conditions such as the outer and inner diameter of the bearing, bearing material properties, and the axial displacement *Δx* as required in the application. These parameters are determined by the situation and are dependent on the application. The designer's parameters, on the other hand, are all other parameters of the bearing that determine the stiffness and endurance life, such as:

- the number of arms *n*
- the arm turn angle θ
- the thickness *t*
- the slot width *s*
- the ending hole diameter *d*

These parameters can be found by the designer during the selection process.

The bearing design tool developed in the following sections is divided into three distinct steps. The first step allows the designer to determine the arm width of the bearing for 2, 3 or 4 arms, for a given ratio of displacement to outer diameter, and for an available sheet metal thickness. The second step yields the value of the stiffness ratio. By comparing this ratio for each number of arms the designer can determine the final number of arms. The third step uses the obtained arm width to determine the pitch of the bearing and the turn angle of the spiral corresponding to this pitch.

The user-specific geometric dimensions are made dimensionless by dividing each by the outer diameter. The outer diameter was chosen because it is the predominant constraint in

the design of a Stirling machine in this context. For example, the outer diameter of the flexure bearing may be chosen based on the cylinder diameter. In order to simplify this process the slot width and the starting hole diameter should be pre-selected, although they can be refined at a later stage using finite element analysis. The charts in Figure 16 are based on the results from FE analysis where the maximum stresses were kept below the endurance limit and are plotted for an ultimate tensile strength of 1.4 GPa as a reference, which is a typical value for stainless spring steels. For any other material, the respective ultimate tensile strength needs to be divided by this reference. This ratio will then need to be multiplied by $\Delta x/OD$ as indicated in the first step chart. The selection process and the use of the charts is explained with the following example. The numbers refer to Figure 16.

First step:

The first step needs to be carried out for 2, 3 and 4 arms each (only 2 arms shown here). It allows the designer to determine the arm width of the bearing while meeting the requirement for infinite life. For an available or convenient sheet metal thickness (1) and a given $\Delta x/OD$ ratio a horizontal line can be drawn (2) until the line intersects with the respective t/OD curve. If this line crosses the thickness curve twice the designer may choose the largest arm width. This intersection point determines the w/OD ratio and therefore the arm width w (3). The final number of arms will then be determined in the second step.

As seen earlier in this study, the stiffness ratio increases with the thickness and the arm width. If there is more than one possible solution, the designer is free to select a different thickness depending on whether the focus is more on the radial or axial deformation. At the end of this step the designer has a thickness and an arm width value for each number of arms.

Second step:

In this step the stiffness ratio is calculated as a function of the arm width and the thickness based on Wahl's correlation [12]:

$$\frac{k_r}{k_a} = \frac{1.7}{k_3} * \frac{\left(\frac{w}{OD}\right)^3}{\left(\frac{t}{OD}\right)^2 \left(\frac{w}{OD} - 0.26\frac{t}{OD}\right)} \tag{4}$$

This correlation is the most accurate one for the calculation of the stiffness ratio as described previously. The constant k_3 varies from 1.22 to 1.4 for w/t ratios between 5 and infinity, which is the case for flat arms.

20

In this graph the stiffness ratio can be found on the vertical axis (6) for the *w/OD* value (5) found in the first step, for the selected bearing thickness (4), i.e. the *t/OD* ratio that all the curves in this graph are plotted for.

Third step:

In the third step the designer finds the pitch of the bearing leading to the selection of the turn angle of the bearing The line that is denoted by '2 arms' represents the dimensionless pitch as a function of the *w/OD* ratio and was created by using the following correlation:

$$\frac{w}{OD} = \frac{\frac{p}{OD}}{k} - \frac{s}{OD} \ . \tag{5}$$

Also plotted in this graph are the curves for different turn angles in degrees as a function of the *ID/OD* ratio based on the following relationship:

$$\frac{p}{OD} = \frac{1 - \frac{ID}{OD} - 2\frac{s}{OD}}{\frac{2\theta}{360}}. \tag{6}$$

Where the vertical *w/OD* line intersects with the diagonal '2 arms' line (7), a horizontal line can be drawn. The dimensionless pitch can be found on the vertical axis (8). Finally, for a given *ID/OD* ratio a vertical line can be drawn (9) and a suitable turn angle can be found nearby the intersection with the previously drawn horizontal line (10). In the given example, a turn angle of 540° appears to be suitable.

At the end of this step all the geometric dimensions of the bearing have been found. A final rapid finite elements analysis may be carried out to refine the slot width and the starting hole diameter in order to check the exact stress values, and the radial and axial stiffness of this configuration.

(Footnote: Proper diagrams in pdf-format can be emailed by the corresponding author on request.)
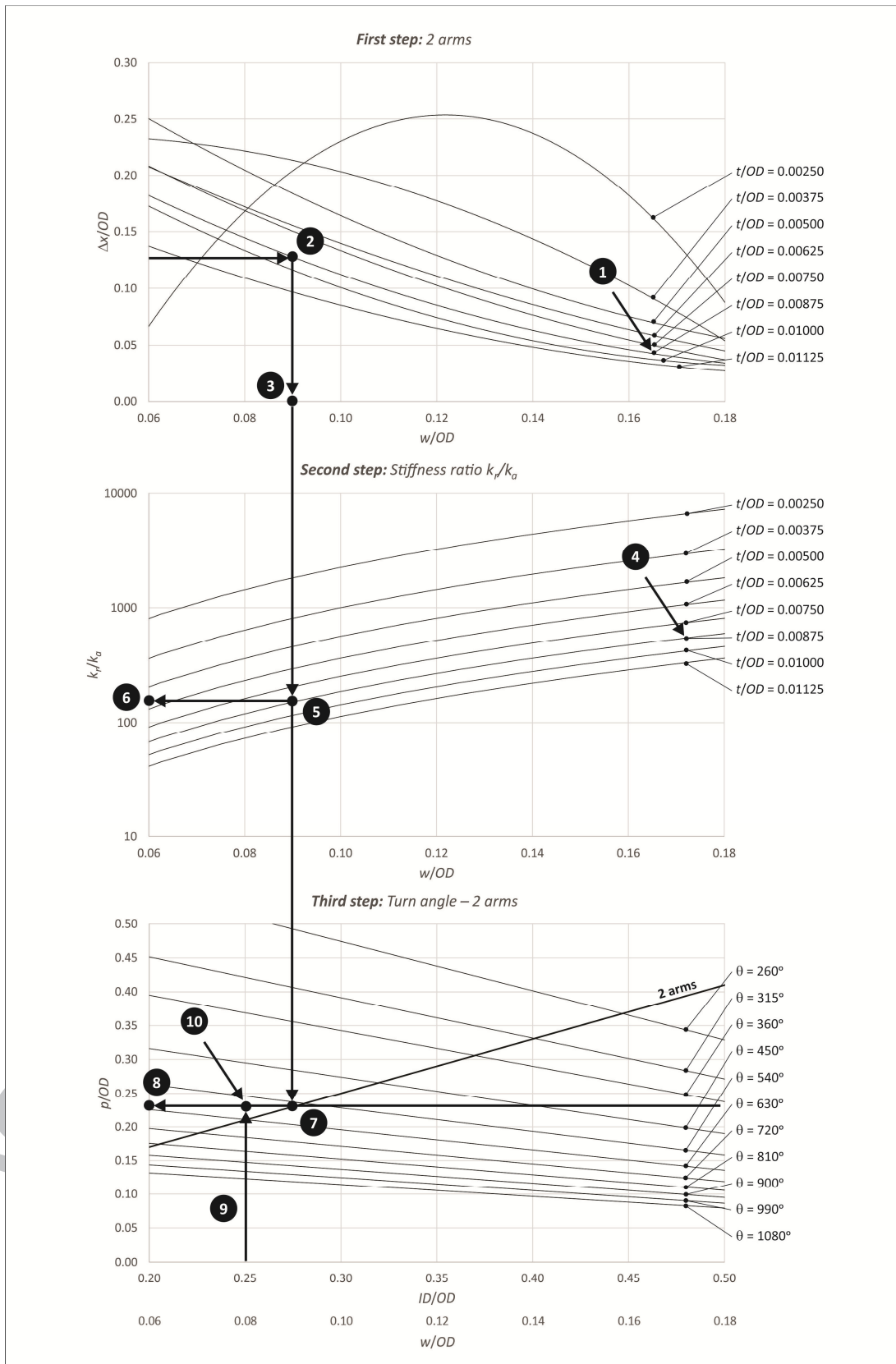
Figure 16: Design method example for a two arms flexure bearing with $\Delta x/OD$ = 0.125.

Conclusion

The geometric parameters of a flexure bearing were varied in a FEM analysis in order to determine their influence on axial and radial stiffness, as well as on maximum occurring stresses. A dynamic and modal analysis was carried out to identify the best geometric parameters for infinite life of the bearing at a highest possible radial to axial stiffness ratio. The approach presented here can be applied to optimising other flexure bearings with different specifications. A graphical design tool has been developed to assist designers to select a proper bearing configuration for a given situation. This design method allows designers to quickly pre-dimension a flexure bearing; however, a FE analysis is still recommended once the geometric parameters have been chosen to further refine the performance values since this approach is based on some simplifying assumptions.

The results of this study are summarised as follows:

- The natural frequency of the bearing decreases with the turn angle and number of arms of the spiral.
- The stiffness ratio is a useful design criterion to evaluate the performances of flexure bearings; it decreases with the turn angle and the number of arms. This ratio can be improved by increasing the arm width and reducing the thickness of the bearing.
- The stresses of the bearing are concentrated at the starting holes of the spiral. These stresses can be reduced by increasing the number of arms and the turn angle of the spiral, or by reducing the bearing thickness and the arm width.
- Flexure bearing design is a compromise between the stiffness ratio and the maximum stresses at the starting holes.
- The new graphical design method presented here is a useful tool for flexure bearing pre-dimensioning that can be directly used for any stainless steel spring material, or apportioned by ratio of ultimate strength for any other spring material, and any common configuration; although a FE analysis is recommended after this process to further refine bearing performance.

References

[1] Wolf A. et al., 1938, Vibration Detector US Patent N. 2,130,213.

[2] Davey, C., "The Oxford University Miniature Cryogenic Refrigerator", International Conference on Advanced infrared Detectors and Systems, London, 1981, 39.

[3] Wong, T.E., Pan R.B. and Johnson A.L., "Novel linear flexure bearing", in: Proc 7th Int Cryo Conf, 1992, 675-698.

[4] Marquardt, E., Radebaugh, R. and Kittel, P., "Design equations and scaling laws for linear compressors with flexure springs", in: Proc 7th Int Cryo Conf, 1992, 783-804.

[5] Wong T.E., Pan R.B., Marten H.D., Sve C., Galvan L. and Wall T.S. "Spiral flexural bearing" in: Proc 8th Cryo Conf , 1995, 305-311.

[6] Gaunekar A. S., Goddenhenrich T., Heiden C., "Finite element analysis and testing of flexure bearing elements", in: Cryogenics 36, 1996, 359–364.

[7] Lee C. C. and Pan R. B., "Flexure bearing analysis procedures and design charts", in: Cryocoolers 9, Plenum Press, New York, 1997, 413-420.

[8] Al-Otaibi Z. S., Jack A. G., "Spiral flexure springs in single phase linear-resonant motors", in: Proceeding of: 42nd International Universities Power Engineering Conference (UPEC 2007), 184-187.

[9] Simcock C. J., "Investigation of materials for long life, high reliability flexure bearing spring for Stirling Cryocooler Applications", in: Cryocoolers 14, 2007, 335-343.

[10] Malpani S., Yenarkar Y., Deshmukh S., Tak S. P., Bhope D.V., "Design of flexure bearing for linear compressor by optimization procedure using FEA" in: International Journal of Engineering Science and Technology (IJEST), Vol. 4 No.05 May 2012, 1991-1999.

[11] Kavade M.V., Patil C.B., "Optimization of flexure bearing using FEA for linear compressor", International Journal of Engineering and Science (IJEST), Vol. 1, Issue 12 December 2012, 37-45.

[12] Wahl A. M., Mechanical Springs, McGraw-Hill, 1963.

[13] Gedeon D., Sage User's Guide, 2014, 162-167.

[14] Shigley J. E., Mechanical Engineering Design, 1972, 243-270.

Parameter study and design optimisation of a flexure bearing

Simon Amoedo[1], Michael Gschwendtner[2] and David White[2]

[1]ISAE-ENSMA, France

[2]Department of Mechanical Engineering, Auckland University of Technology, New Zealand

Corresponding author:

Michael Gschwendtner, School of Engineering, Private Bag 92006, Auckland 1142, New Zealand.

Email: michael.gschwendtner@aut.ac.nz

Highlights

- Modal analysis of the flexure bearing for the different designs are performed.
- Dynamic tests on the flexure bearing are carried out using finite element method.
- We study the influence of new geometry parameters on the performances of the bearing.
- A final design of the flexure bearing is chosen for a specific application.

Abstract

The objective of this study was to design and optimise a flexure bearing to be used in a Stirling engine with a fixed axial displacement and a fixed outer diameter. This was achieved through a parameter study of the bearing carried out with ANSYS®. The parameters varied were the number and the width of the arms, the thickness of the bearing, the eccentricity, the size of the starting and ending holes, and the number of turns of the spiral. Comparison was made between the different designs in terms of axial and radial stiffness, the natural frequency, and the maximum induced stresses. Moreover, the Finite Element Analysis (FEA) was compared to theoretical results for a given design. Results demonstrate that both the natural frequency and the stiffness ratio decrease with the number of turns and arms, and that eccentricity and section variation do not significantly improve the performance of the bearing in terms of the stiffness ratio and maximum stresses.